Jets at NNLO: status and use in PDF's

João Pires*
Universita degli Studi di Milano
INFN sezione di Milano

15-21 February 2015 Benasque, Spain

Inclusive jet and dijet cross sections

- look at the production of jets of hadrons with large transverse energy in
  - inclusive jet events $pp \to j + X$
  - exclusive dijet events $pp \to 2j$

- cross sections measured as a function of the jet p_T, rapidity y and dijet invariant mass m_{jj} in double differential form

$$\frac{\mathrm{d}^2\sigma}{\mathrm{d}p_T\mathrm{d}y} = \frac{1}{\epsilon\mathscr{L}_{\mathrm{eff}}}\frac{N_{\mathrm{jets}}}{\Delta p_T\,(2\cdot\Delta|y|)}$$

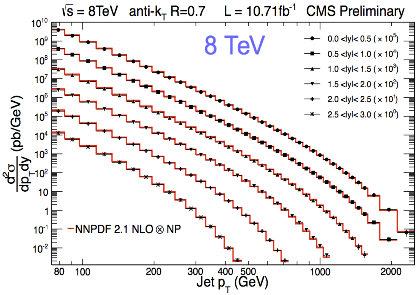

CMS PAS SMP-12-012

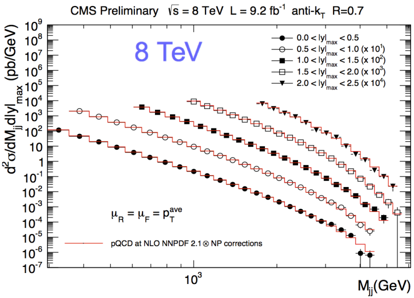

CMS-PAS-SMP-14-002

Inclusive jet cross section

- Jets up to $|y| = 3.0$, $p_T = 2.5$ TeV. Six rapidity bins of $\Delta|y| = 0.5$. @ 8TeV

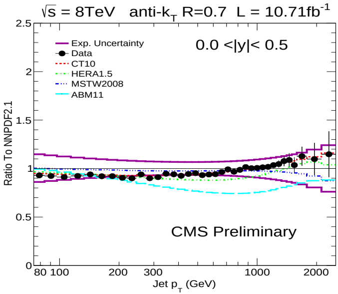

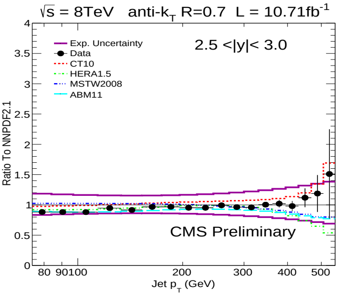

- theory: NLO QCD$\otimes$NP
- overall good agreement with data with similar predictions at low-p_T
  - except ABM11 $\rightarrow$ not included jet data in their fit since NNLO corrections may be large
- significant mismatch in the predictions at high-p_T between all sets

$$\begin{aligned} \delta_{experimental} &\sim 15-40\% \quad (\text{JES, luminosity, unfolding}) \\ \delta_{theory} &\sim 10-50\% \quad (\text{PDF}, \mu_R, \mu_F) \end{aligned}$$

Dijet cross section

- Jets up to $|y| = 2.5$, $M_{jj} = 5.5$ TeV. Six rapidity bins of $\Delta|y_{\max}| = 0.5$. @ 8TeV

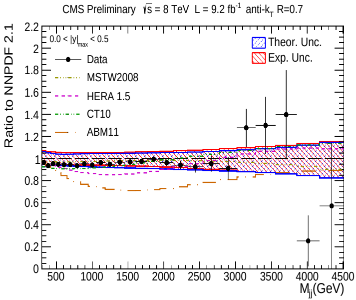

CMS-PAS-SMP-14-002

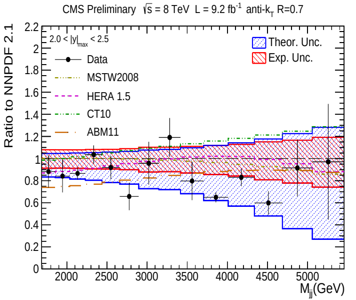

CMS-PAS-SMP-14-002

- overall good agreement with data within statistical/systematical uncertainties in all rapidity bins
- theory predictions show differences of $\mathscr{O}(10\%)$
- theoretical and experimental uncertainties are of comparable size even at high M_{jj}

$$
\begin{aligned}
\delta_{experimental} &\sim 5-20\% \quad (\text{JES, luminosity, unfolding}) \\
\delta_{theory} &\sim 5-40\% \quad (\text{PDF}, \mu_R, \mu_F)
\end{aligned}
$$

Towards NNLO QCD

Motivation for NNLO

- to include higher-order effects $\rightarrow$ only way to reduce theoretical uncertainties in the fixed-order predictions used in experimental analysis
- to make reliable theory comparisons with LHC jet data
- to make jet data consistently included in NNLO PDF fits

Towards NNLO QCD

Motivation for NNLO

- to include higher-order effects $\rightarrow$ only way to reduce theoretical uncertainties in the fixed-order predictions used in experimental analysis
- to make reliable theory comparisons with LHC jet data
- to make jet data consistently included in NNLO PDF fits

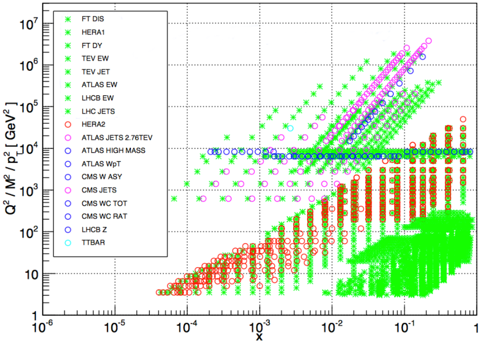

(NNPDF collaboration)

- particularly sensitive to gluon PDF at medium and large values of x $\rightarrow$ reduce PDF uncertainty
- different data constrain different parton combinations at different x
- check NNLO consistency with HERA, DIS and Tevatron data
- check consistency with $t\bar{t}$ data

Inclusive jet and dijet cross sections

<u>State of the art:</u>

- dijet production is known in NLO QCD
  [Ellis, Kunszt, Soper ’92]
  [Giele, Glover, Kosower ’94], [Nagy ’02]
- NLO+Parton shower
  [Alioli, Hamilton, Nason, Oleari, Re ’11]
- NLO EW corrections
  [Dittmaier, Huss, Speckner ’12]
- approximate NNLO threshold corrections
  [Kidonakis, Owens ’00], [Florian, Hinderer, Mukherjee, Ringer, Vogelsang ’13]

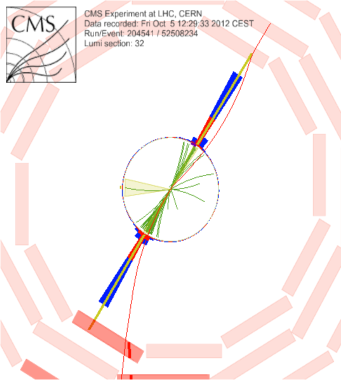

$\mathrm{M}_{jj} = 5.5$ TeV

<u>Goal:</u>

- obtain the jet cross sections at NNLO exact accuracy in double differential form

$$\frac{\mathrm{d}^2\sigma}{\mathrm{d}p_T\mathrm{d}|y|} \qquad \frac{\mathrm{d}^2\sigma}{\mathrm{d}m_{jj}\mathrm{d}y^*}$$

NNLO ingredients

QCD jet cross section perturbative expansion at hadron colliders

$$d\sigma = \sum_{i,j} \int \left[d\hat{\sigma}_{ij}^{LO} + \left(\frac{\alpha_s}{2\pi}\right) d\hat{\sigma}_{ij}^{NLO} + \left(\frac{\alpha_s}{2\pi}\right)^2 d\hat{\sigma}_{ij}^{NNLO} + \mathcal{O}(\alpha_s^3) \right] f_i(x_1) f_j(x_2) dx_1 dx_2$$

NNLO m-jet correction contains three contributions:

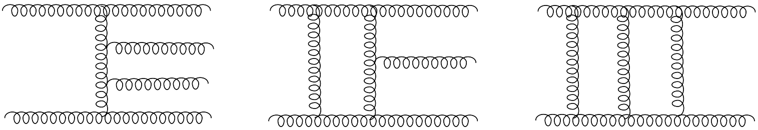

$$d\hat{\sigma}_{NNLO} = \int_{d\Phi_4} d\hat{\sigma}_{NNLO}^{RR} + \int_{d\Phi_3} d\hat{\sigma}_{NNLO}^{RV} + \int_{d\Phi_2} d\hat{\sigma}_{NNLO}^{VV}$$

- explicit infrared poles from loop integrations
- implicit poles in phase space regions for single and double unresolved gluon emission
- procedure to extract the infrared singularities and assemble all the parts in a parton-level generator
- differential cross sections→ kinematics of the final state intact to apply arbitrary phase space observable cuts

NNLO antenna subtraction

$$\begin{aligned} d\hat{\sigma}_{NNLO} &= \int_{d\Phi_4} \left(d\hat{\sigma}^{RR}_{NNLO} - d\hat{\sigma}^{S}_{NNLO} \right) + \int_{d\Phi_3} \left(d\hat{\sigma}^{RV}_{NNLO} - d\hat{\sigma}^{T}_{NNLO} \right) \\ &+ \int_{d\Phi_2} \left(d\hat{\sigma}^{VV}_{NNLO} - d\hat{\sigma}^{U}_{NNLO} \right) \end{aligned}$$

- extract singularities keeping the kinematics of the final state intact
- IR pole cancellation analytic and local in phase space

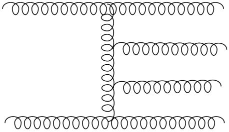

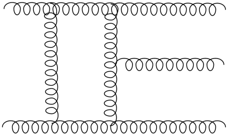

- double unresolved configurations
  - double soft
  - triple collinear
  - double collinear
  - single soft and single collinear
- single unresolved configurations
  - single soft
  - single collinear
- remove overlapping of various single and double soft and/or collinear limits

leading-N_F contributions at NNLO

NNLO contributions	perturbative order
$gg \to q\bar{q}gg$	tree-level (RR)
$gg \to q\bar{q}g$	one-loop (RV)
$gg \to ggg$	one-loop (RV)
$gg \to gg$	two-loop (VV)
$gg \to q\bar{q}$	two-loop (VV)

$$\mathrm{d}\hat{\sigma}^{RR}_{NNLO} \quad \to \quad \mathrm{d}\hat{\sigma}^{S}_{NNLO}$$
$$\mathrm{d}\hat{\sigma}^{RV}_{NNLO} \quad \to \quad \mathrm{d}\hat{\sigma}^{T}_{NNLO}$$

- 27 independent double/single unresolved singularities at RR level, e.g.,
  - triple collinear final-state $P_{q\bar{q}g} \to g, P_{qgg} \to q$
  - triple collinear initial-state $P_{\hat{g}q\bar{q}} \to \hat{g}, P_{\hat{g}qg} \to \hat{\bar{q}}, P_{\hat{g}gg} \to \hat{g}$
- NLO and NNLO antenna functions correctly approximate the matrix elements in all unresolved configurations

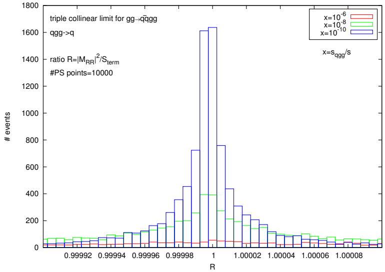

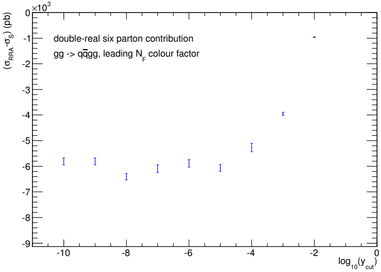

NNLO antenna subtraction - VV process

- VV antenna subtraction term IR pole structure [Currie, Glover, Wells 2013]
  - integrated single unresolved emission from RV process $\propto$ tree-level single soft function

$$\mathscr{P}oles(\mathrm{d}\hat{\sigma}^{U,a}_{NNLO}) \quad \sim \quad \mathbf{J^1}(\epsilon, \hat{1}_g, \hat{2}_g, i_g, j_g)\Big(A^1_4(\hat{\hat{1}}_g, \hat{\hat{2}}_g, i_g, j_g) - \frac{b_0}{\epsilon} A^0_4(\hat{\hat{1}}_g, \hat{\hat{2}}_g, i_g, j_g)\Big)$$

  - integrated iterated NLO emissions of RR process in analytic one-to-one correspondence with $(\mathbf{I}^1)^2$ operator of Catani

$$\mathscr{P}oles(\mathrm{d}\hat{\sigma}^{U,b}_{NNLO}) \quad \sim \quad \mathbf{J^1}(\epsilon, \hat{1}_g, \hat{2}_g, i_g, j_g) \otimes \mathbf{J^1}(\epsilon, \hat{1}_g, \hat{2}_g, i_g, j_g) A^0_4(\hat{\hat{1}}_g, \hat{\hat{2}}_g, i_g, j_g)$$

  - integrated double unresolved emission of RR process $\propto$ tree-level double soft function
  - integrated single unresolved emission of RV process $\propto$ one-loop single soft function
  - when added are in analytic one-to-one correspondence with $\mathbf{I}^2$ operator of Catani

$$\mathscr{P}oles(\mathrm{d}\hat{\sigma}^{U,c}_{NNLO}) \quad \sim \quad \mathbf{J^2}(\epsilon, \hat{1}_g, \hat{2}_g, i_g, j_g)\, A^0_4(\hat{\hat{1}}_g, \hat{\hat{2}}_g, i_g, j_g)$$

- double virtual antennae subtraction term $\mathrm{d}\hat{\sigma}^{U}_{NNLO}$ written compactly rederives the predicted Catani pole structure of the two-loop contribution in the antennae language

leading-N_F VV contribution $gg \to gg$

- all independent double/single unresolved singularities at RR, RV level, collapse to a simple structure once integrated down to the VV level

$$\begin{aligned} \mathrm{d}\sigma_U &= \hat{\mathbf{J}}_4^1(1_g,2_g,i_g,j_g)A_4^1(1_g,2_g,i_g,j_g) \\ &+ \mathbf{J}_4^1(1_g,2_g,i_g,j_g)\hat{A}_4^1(1_g,2_g,i_g,j_g) \\ &+ \mathbf{J}_4^1(1_g,2_g,i_g,j_g)\otimes\hat{\mathbf{J}}_4^1(1_g,2_g,i_g,j_g)A_4^0(1_g,2_g,i_g,j_g) \\ &+ \hat{\mathbf{J}}_4^2(1_g,2_g,i_g,j_g)A_4^0(1_g,2_g,i_g,j_g) \end{aligned}$$

- allowing us to define integrated dipoles (in one-to-one correspondence with IR-Catani pole operators) with an analytic expansion in $d = 4 - 2\epsilon$ for all possible flavour combinations, e.g.,

$$\begin{aligned} \hat{\mathbf{J}}_4^2(1_g,2_g,i_g,j_g) &= \hat{\mathbf{J}}_2^2(\hat{1}_g,\hat{2}_g)+\hat{\mathbf{J}}_2^2(\hat{2}_g,i_g)+\hat{\mathbf{J}}_2^2(i_g,j_g)+\hat{\mathbf{J}}_2^2(j_g,\hat{1}_g) \\ &\to \text{leading-}N_F \text{ FF, IF, II gluon-gluon dipoles} \end{aligned}$$

$$\begin{aligned} \hat{\mathbf{J}}_2^2(\hat{1}_g,\hat{2}_g) &= \mathscr{G}_{4,gg}^0(s_{12}) + \hat{\mathscr{F}}_3^1(s_{12}) + \frac{b_F}{\epsilon}\mathscr{F}_3^0(s_{12})\left(\left(\frac{|s_{12}|}{\mu^2}\right)^{-\epsilon}-1\right) - \frac{1}{2}\bar{\Gamma}_{gg,F}^2(z_1) - \frac{1}{2}\bar{\Gamma}_{gg,F}^2(z_2) \\ &+\frac{1}{2}\frac{b_F}{\epsilon}\Gamma_{gg}^1(z_1) + \frac{1}{2}\frac{b_F}{\epsilon}\Gamma_{gg}^1(z_2) + \frac{1}{2}\frac{b_0}{\epsilon}\hat{\Gamma}_{gg}^1(z_1) + \frac{1}{2}\frac{b_0}{\epsilon}\hat{\Gamma}_{gg}^1(z_2) \\ &+S_{g\to q}\Gamma_{qg}(z_1)\mathscr{G}_{3,qg}^0(s_{12}) + S_{g\to q}\Gamma_{qg}(z_2)\mathscr{G}_{3,gq}^0(s_{12}) + \frac{1}{2}\Gamma_{gq}^1(z_1)\Gamma_{qg}^1(z_1) + \frac{1}{2}\Gamma_{gq}^1(z_2)\Gamma_{qg}^1(z_2) \end{aligned}$$

leading-N_F VV contribution $gg \to q\bar{q}$

- Similarly,

$$\begin{aligned}
\mathrm{d}\sigma_U &= \mathbf{J}_4^1(i_q,1_g,2_g,j_{\bar{q}})B_2^1(i_q,1_g,2_g,j_{\bar{q}}) \\
&+ \frac{1}{2}\mathbf{J}_4^1(i_q,1_g,2_g,j_{\bar{q}}) \otimes \mathbf{J}_4^1(i_q,1_g,2_g,j_{\bar{q}})B_2^0(i_q,1_g,2_g,j_{\bar{q}}) \\
&+ \mathbf{J}_4^2(i_q,1_g,2_g,j_{\bar{q}})B_2^0(i_q,1_g,2_g,j_{\bar{q}}) \\
&- \bar{\mathbf{J}}_4^2(i_q,1_g,2_g,j_{\bar{q}})B_2^0(i_q,1_g,2_g,j_{\bar{q}})
\end{aligned}$$

- allowing us to define the integrated dipoles, $J_2^{(2)}(q,\hat{g})$, $\bar{J}_2^{(2)}(q,\hat{g})$ such that IR pole cancellation between real and virtual corrections at NNLO is achieved in transparent and analytic way

$$\boxed{\mathscr{P}oles\left(\mathrm{d}\hat{\sigma}^{VV}_{NNLO} - \mathrm{d}\hat{\sigma}^{U}_{NNLO}\right) = 0 \qquad \text{for } gg \to q\bar{q}}$$

Advantages,

- integrated dipoles are process independent
- need to be derived once and for all and then can be recycled to compute other processes at NNLO
- calculation organized in a way that naturally leads to automation of the method

Jet production partonic channels

Fraction of jets per initial state contribution

LHC

- $gg \to gg$ dominates at low p_T
- $qg \to qg$ important in all p_T regions
- $qq \to qq$ dominant at high p_T

Tevatron

- qg and $q\bar{q}$ dominant

Numerical results at NNLO for

- $gg \to gg$ at leading colour
- $gg \to gg$ at subleading colour
- $q\bar{q} \to gg$ at leading colour

Ongoing work

- numerical implementation of qg and qq dipoles to extract predictions for qg and qq initial states

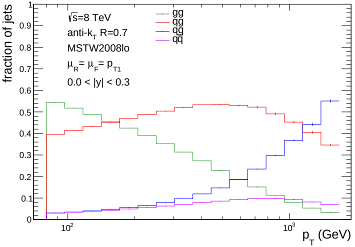

(LHC 8 TeV)

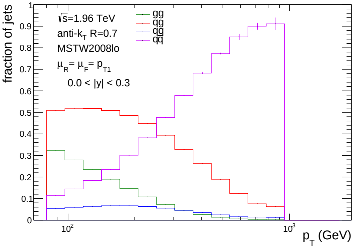

(Tevatron 1.96 TeV)

Numerical setup

- pp collisions at $\sqrt{s} = 8$ TeV
- jets identified with the anti-k_T jet algorithm with resolution parameter $R = 0.7$
- jets accepted at rapidities $|y| < 4.4$
- leading jet with transverse momentum $p_T > 80$ GeV
- subsequent jets required to have at least $p_T > 60$ GeV
- MSTW2008nnlo PDF for all fixed-order predictions
- dynamical factorization and renormalization scales equal to the leading jet p_T $(\mu_R = \mu_F = \mu = p_{T1})$
- present results for full colour $gg \to gg$ scattering and $q\bar{q} \to gg$ leading colour combined at NNLO

Inclusive jet p_T distribution at NNLO

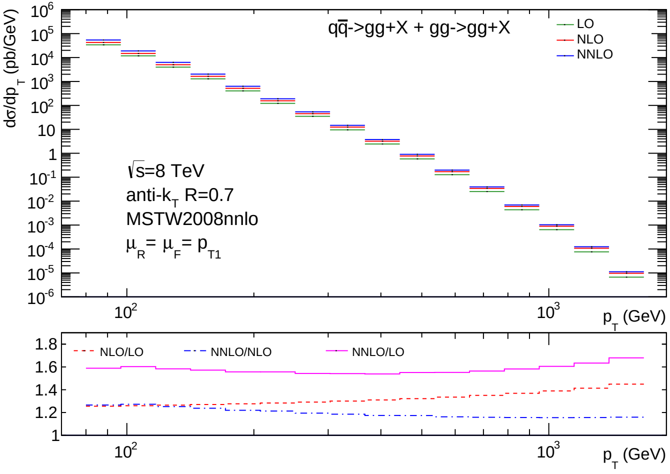

- all jets in an event are binned
- NNLO correction stabilizes the NLO k-factor growth with p_T
- NNLO corrections $15 - 26\%$ with respect to NLO

Double differential inclusive jet p_T distribution at NNLO

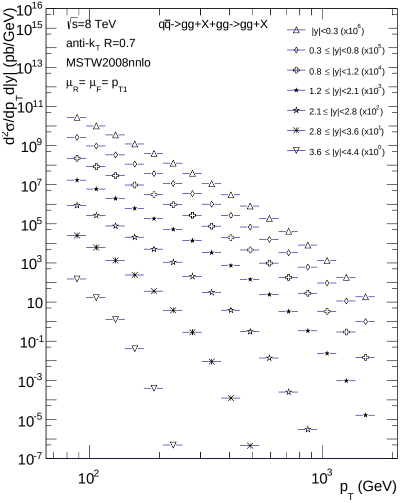

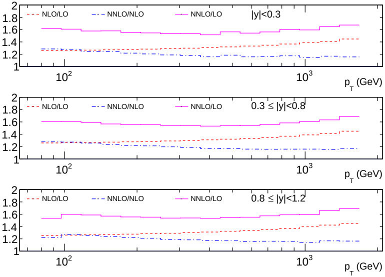

double differential k-factors

- NNLO prediction increases between 25% to 15% with respect to the NLO cross section
- similar behaviour between the rapidity slices

Scale choice for theory prediction

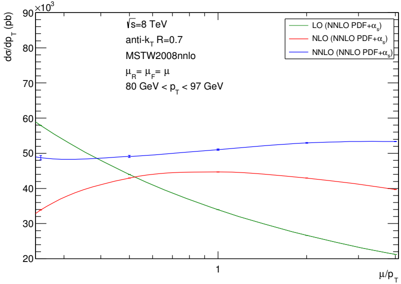

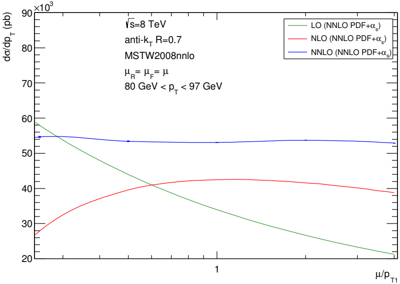

- scale dependence of the theory prediction gg-channel much reduced at NNLO
- size of the correction and uncertainty at low-p_T still depends on scale choice P_{T1} vs P_T

Double differential exclusive dijet mass distribution at NNLO

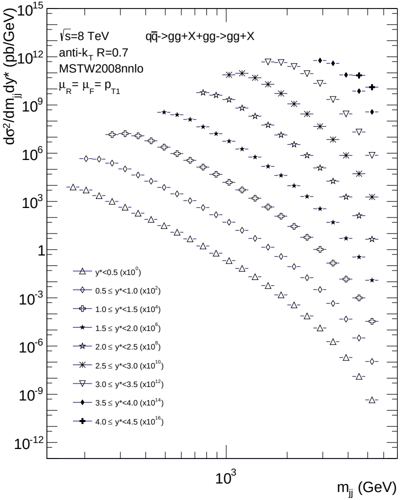

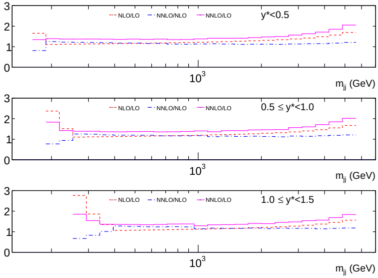

double differential k-factors

- NNLO corrections up to 20% with respect to the NLO cross section
- similar behaviour between the $y^* = 1/2|y_1 - y_2|$ slices
- asymmetric p_T cut for leading and subleading jet

Comparison with approximate NNLO predictions

- Approximate NNLO results from an improved threshold calculation for the single jet inclusive production [de Florian, Hinderer, Mukherjee, Ringer, Vogelsang '13]
  - $pp \to j + X$ with the threshold limit given by $s_4 = P_X^2 \to 0$
  - near threshold phase space available for real-gluon emission is limited
  - higher kth order coefficient functions dominated by large logarithmic corrections

$$\alpha_s^k w_{ab}^{(k)} \to \alpha_s^k \left(\frac{\log^m(z)}{z} \right)_+ , \qquad m \leq 2k-1, \qquad z = \frac{s_4}{s}$$

  - $\delta(z)$ ✗, 4th tower ✗, $\mathscr{O}$(z) ✗

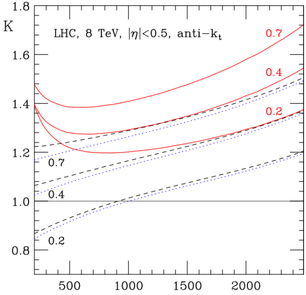

(all-channels)

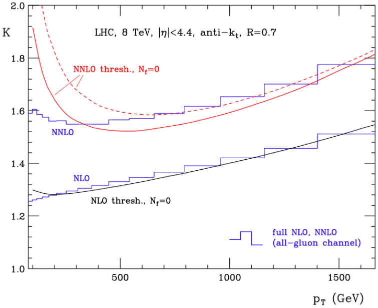

(gluons only channel) - rapidity integrated

NNLO benchmark predictions for jet production

S. Carrazza, JP, arXiv:1407.7031

- understand and characterise the validity of the NNLO threshold approximation by comparing it with the exact computation using the gg-channel
- $\mu_R = \mu_F = p_T$ for both predictions
- comparison performed differential in p_T and rapidity following the exact experimental setups
- NNPDF23_nnlo_as_0118 set for all fixed order predictions
- NLO benchmark curves
  - green dashed curves $\rightarrow$ NLO-threshold gg-channel
  - black dashed curves $\rightarrow$ NLO-exact gg-channel
  - blue dashed curves $\rightarrow$ NLO-exact all channels
- NNLO benchmark curves
  - pink long-dashed curves $\rightarrow$ NNLO-threshold gg-channel $\rightarrow$ $\boxed{\mathrm{d}\sigma^{\mathrm{thresh}}_{gg,NNLO}/\mathrm{d}\sigma_{gg,LO}}$
  - black long-dashed curves $\rightarrow$ NNLO-exact gg-channel $\rightarrow$ $\boxed{\mathrm{d}\sigma^{\mathrm{exact}}_{gg,NNLO}/\mathrm{d}\sigma_{gg,LO}}$

Tevatron CDF Run-II $\sqrt{s}$=1.96 TeV

S. Carrazza, JP, arXiv:1407.7031

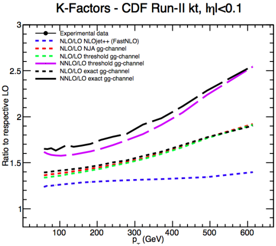

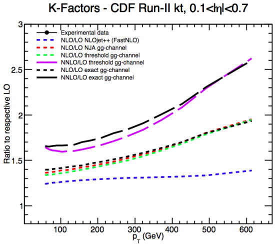

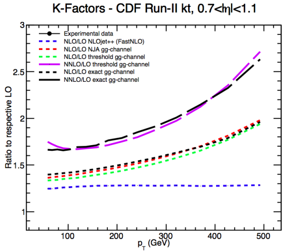

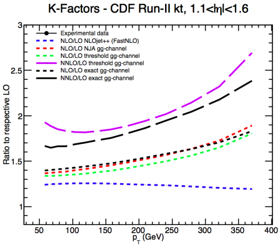

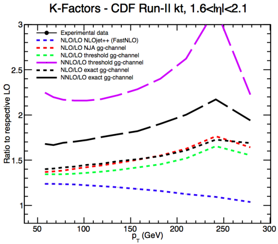

- differences $\leq$ 15% at low-p_T in the central regions
- in the forward region differences $\geq$40% for all p_T regions

LHC ATLAS 2010 $\sqrt{s}$=7 TeV

S. Carrazza, JP, arXiv:1407.7031

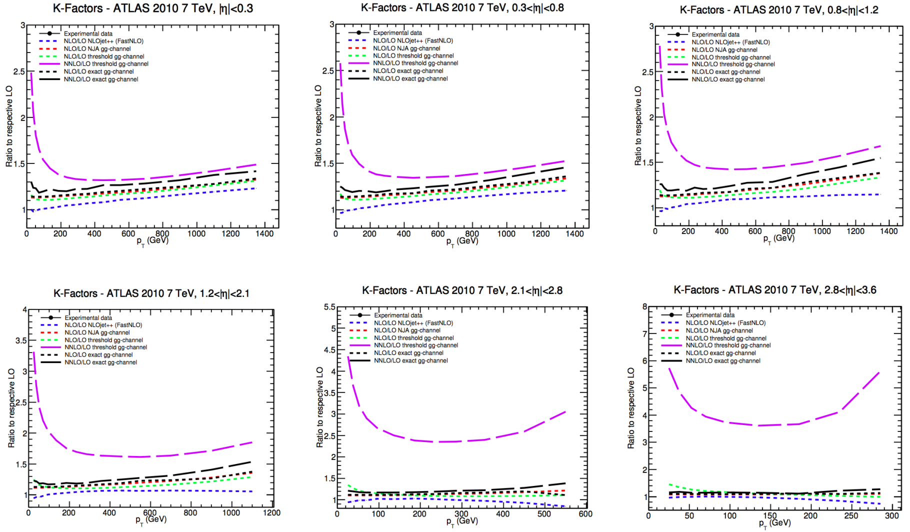

- differences large at small p_T and increase with rapidity
- exact NNLO k-factor decreases with rapidity, NNLO threshold k-factor increases with rapidity

Threshold approximation - gg channel

S. Carrazza, JP, arXiv:1407.7031

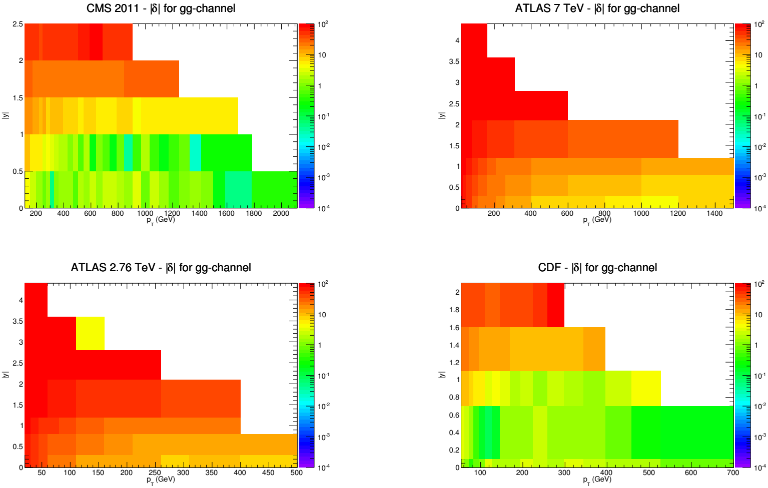

- relative difference $|\delta|$ between exact and approximate gg-channel k-factors as a function of p_T and $|y|$ for CMS, ATLAS 7 TeV and 2.76 TeV and CDF bins

Gluon-PDF

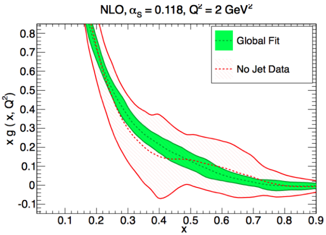

NNPDF collaboration

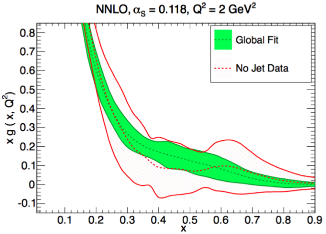

NNPDF collaboration

- jet data has a big impact on the medium to large-x gluon PDF reducing its uncertainty
- fit at NNLO obtained using a $|\delta| < 10\%$ criteria which excluded many jet data
- need exact NNLO all-channel prediction to include full jet dataset

Conclusions

- jet cross sections at the LHC delivered with increasing experimental accuracy making jet measurements precision physics
- double-differential jet measurements have a big impact on the extraction of the gluon PDF at medium to large-x
- experimental and theory errors of comparable size
- presented exact results for $gg \to gg + X$ and $q\bar{q} \to gg + X$ at NNLO
- leading-N_F gg RR, RV and VV corrections derived
- perfomed comparison between exact NNLO results and approximate NNLO results from threshold resummation in the gg-channel
  - largest differences arise at low-p_T for central rapidities and all p_T at large rapidities
  - differences are smaller at the Tevatron than at the LHC 7 TeV

Ongoing work:

- numerical implementation of qg and qq integrated dipoles to extract predictions for qg and qq initial states
- qg channel - most important at the LHC
- qq channel - important at high p_T

Back-up slides

Threshold approximation - gg channel

S. Carrazza, JP, arXiv:1407.7031

CMS 2011	N_{dat}	χ^2/dof	Exclusion regions (y, p_T)	
$\|\delta\| < 15\%$	88	1.81	$1.0 < \|y\| < 1.5$	$p_T < 153$ GeV
			$\|y\| > 1.5$	all p_T bins
$\|\delta\| < 10\%$	83	1.89	$1.0 < \|y\| < 1.5$	$p_T < 272$ GeV
			$\|y\| > 1.5$	all p_T bins
$\|\delta\| < 7.5\%$	77	1.89	$0.5 < \|y\| < 1.0$	$p_T < 153$ GeV
			$1.0 < \|y\| < 1.5$	$p_T < 395$ GeV
			$\|y\| > 1.5$	all p_T bins
$\|\delta\| < 5\%$	59	1.83	$0.5 < \|y\| < 1.0$	$p_T < 220$ GeV
			$1.0 < \|y\| < 1.5$	$p_T < 737$ GeV, $p_T > 790$ GeV
			$\|y\| > 1.5$	all p_T bins

ATLAS 7 TeV	N_{dat}	χ^2/dof	Exclusion regions (y, p_T)	
$\|\delta\| < 15\%$	16	1.82	$0.0 < \|y\| < 0.3$	$p_T < 260$ GeV
			$0.3 < \|y\| < 0.8$	$p_T < 400$ GeV
			$0.8 < \|y\| < 1.2$	$p_T < 1$ TeV
			$\|y\| > 1.2$	all p_T bins
$\|\delta\| < 10\%$	9	1.58	$0.0 < \|y\| < 0.3$	$p_T < 400$ GeV
			$0.3 < \|y\| < 0.8$	$p_T < 800$ GeV
			$\|y\| > 0.8$	all p_T bins
$\|\delta\| < 7.5\%$	5	2.02	$0.0 < \|y\| < 0.3$	$p_T < 500$ GeV
			$\|y\| > 0.8$	all p_T bins
$\|\delta\| < 5\%$	1	-	$0.0 < \|y\| < 0.3$	$p_T < 1$ TeV, $p_T > 1.2$ TeV
			$\|y\| > 0.3$	all p_T bins

ATLAS 2.76 TeV	N_{dat}	χ^2/dof	Exclusion regions (y, p_T)	
$\|\delta\| < 15\%$	10	2.15	$0.0 < \|y\| < 0.3$	$p_T < 110$ GeV
			$0.3 < \|y\| < 0.8$	$p_T < 210$ GeV
			$\|y\| > 0.8$	all p_T bins
$\|\delta\| < 10\%$	3	0.35	$0.0 < \|y\| < 0.3$	$p_T < 260$ GeV
			$\|y\| > 0.3$	all p_T bins
$\|\delta\| < 7.5\%$	-	-	all $\|y\|$ bins	all p_T bins
$\|\delta\| < 5\%$	-	-	all $\|y\|$ bins	all p_T bins

CDF	N_{dat}	χ^2/dof	Exclusion regions (y, p_T)	
$\|\delta\| < 15\%$	60	2.32	$1.1 < \|y\| < 1.6$	$p_T < 96$ GeV
			$\|y\| > 1.6$	all p_T bins
$\|\delta\| < 10\%$	52	1.86	$1.1 < \|y\| < 1.6$	$p_T < 224$ GeV, $p_T > 298$ GeV
			$\|y\| > 1.6$	all p_T bins
$\|\delta\| < 7.5\%$	48	1.37	$0.7 < \|y\| < 1.1$	$p_T < 72$ GeV
			$\|y\| > 1.1$	all p_T bins
$\|\delta\| < 5\%$	45	1.28	$0.7 < \|y\| < 1.1$	$p_T < 110$ GeV
			$\|y\| > 1.1$	all p_T bins

- Summary of exclusion regions in p_T and rapidity $|y|$ as a function of the relative difference between exact and threshold k-factors for the gluon-gluon channel
- χ^2/dof for aNNLO PDF fits as a function of exclusion criteria $|\delta|$